Results from Neutrino Physics Experiments

David E. Jaffe

FPCP 2010

What I'm going to talk about

Preface:

- "...review the most relevant results from neutrino phyisics experiment..." since FPCP2009.
- From A. de Gouvêa's FPCP2009 talk: "...a summary talk ... to a group of people more interested in quarks than neutrinos."

Outline:

Quarks *vs* Neutrinos
Terrestrial Neutrinos
Solar Neutrinos
Extraterrestrial Neutrinos
Artificial Neutrinos
Global fit

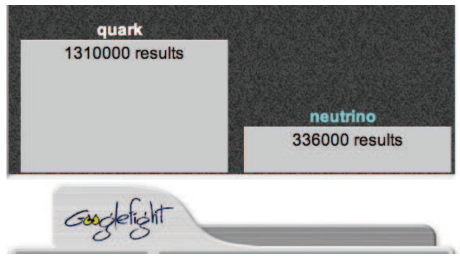

Disclosure: I am a collaborator on MINOS, Daya Bay and LBNE.

Parallels of quarks and neutrinos

3 generations

$$|\psi_i> = \sum_j V^*_{ij}|\psi_j>$$

Cabibbo-Kobayashi-Masakawa	V_{ji}	Pontecorvo-Maki-Nakagawa-Sakata
13°	θ_{12}	34°
2.3°	θ_{23}	43°
0.2°	θ_{13}	$< 12^\circ$ (90% CL)
64.5°	δ	$[0, 360]^\circ$
3×10^{-5}	J	$\leq 3500 \times 10^{-5}$
CKMfitter (Oct09)	ref.	arXiv:1001.4524

Magnitude of CPV $\propto$ Jarlskog invariant [1] $J \equiv Im(V_{ij}V_{kl}V^*_{kj}V^*_{il})$

$$V_{ij} = \begin{pmatrix} c_{12}c_{13} & s_{12}c_{13} & s_{13}e^{-i\delta} \\ -s_{12}c_{23} - c_{12}s_{23}s_{13}e^{i\delta} & c_{12}c_{23} - s_{12}s_{23}s_{13}e^{i\delta} & s_{23}c_{13} \\ s_{12}s_{23} - c_{12}c_{23}s_{13}e^{i\delta} & -c_{12}s_{23} - s_{12}c_{23}s_{13}e^{i\delta} & c_{23}c_{13} \end{pmatrix}$$

where $c_{ij} = \cos\theta_{ij}$, $s_{ij} = \sin\theta_{ij}$ for $i < j = 1, 2, 3$.

[1] Jarlskog, PRL**55**(1985)1039

What we know about neutrino oscillations

$$V_{ij} = \begin{pmatrix} 1 & 0 & 0 \\ 0 & c_{23} & s_{23} \\ 0 & -s_{23} & c_{23} \end{pmatrix} \begin{pmatrix} c_{13} & 0 & s_{13}e^{i\delta} \\ 0 & 1 & 0 \\ -s_{13}e^{-i\delta} & 0 & c_{13} \end{pmatrix} \begin{pmatrix} c_{12} & s_{12} & 0 \\ -s_{12} & c_{12} & 0 \\ 0 & 0 & 1 \end{pmatrix} \begin{pmatrix} e^{i\alpha_1/2} & 0 & 0 \\ 0 & e^{i\alpha_2/2} & 0 \\ 0 & 0 & 1 \end{pmatrix}$$

$\theta_{23} \approx 45^\circ$
Atmospheric ν
Accelerator ν

$\theta_{13} < 12^\circ$
Short-baseline Reactor ν
Future accelerator ν

$\theta_{12} \approx 35^\circ$
Solar ν
Long-baseline Reactor ν

Neutrinoless double beta decay

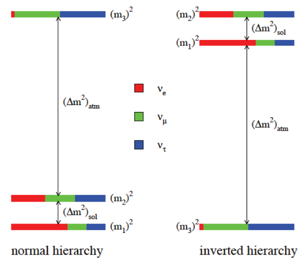

$\Delta m^2_{21} = 7.6 \times 10^{-5}\ \mathrm{eV}^2$ *(solar)*

$|\Delta m^2_{31}| = 2.4 \times 10^{-3}\ \mathrm{eV}^2$ *(atmospheric)*

ν_μ disappearance in 2-ν approximation:

$\mathcal{P}(\nu_\mu \to \nu_\mu) = 1 - \sin^2 2\theta \sin^2(1.27 \Delta m^2 L/E)$

$L(\mathrm{km})$, $E(\mathrm{GeV})$, $\Delta m^2_{ij} \equiv m_i^2 - m_j^2\ (\mathrm{eV}^2)$

Topics and recent neutrino results not discussed

- Neutrinoless Double Beta Decay
- Neutrino mass measurement in ^{3}H decay
- Super-Kamiokande: Search for astrophysical ν point sources. Astrophys.J. **704** (2009) 503.
- MiniBooNE: Measurement of ν_μ CC quasielastic double differential cross section. arXiv:1002.2680
- MiniBooNE: Measurement of ν_μ and $\bar{\nu}_\mu$ NC single π^0 production cross section on mineral oil at $E_\nu \sim \mathcal{O}(1\ \mathrm{GeV})$. PRD**81** (2010) 013005.
- MINOS: ν_μ and $\bar{\nu}_\mu$ inclusive CC cross-sections. arXiv:0910.2201
- MINOS: Search for sterile neutrino mixing. arXiv:1001.0336

Borexino: Observation of geo-neutrinos arXiv:1003.0284

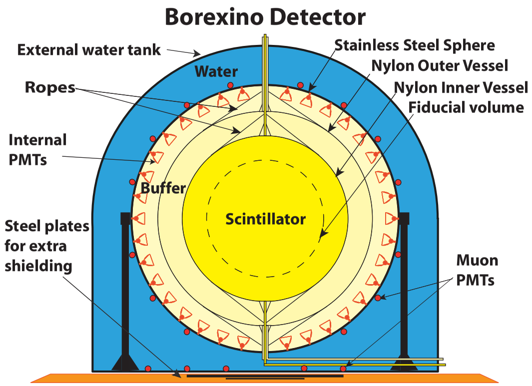

- Located in LNGS, 3800 m.w.e. overburden
- 278 tons target of high-purity liquid scintillator (8.5m diam. inner vessel)
- 890 tons buffer (11.5m outer vessel, 13.7m SS shell)
- Target viewed by 2212 8" PMTs
- Water-filled external tank, viewed by 208 8" PMTs
- Exposure: 253 ton·year

Borexino: Detection of geo-neutrinos

- Geo-neutrinos are $\bar{\nu}_e$ produced by β decays of $^{40}\mathrm{K}$ and nuclides in the $^{238}\mathrm{U}$ and $^{232}\mathrm{Th}$ chains.
- Provide a direct measure of abundance and distribution of radioactive elements in the Earth, and would permit an assessment of the radiogenic contribution of the Earth's heat balance.
- $\bar{\nu}_e$ are detected via inverse beta decay $\bar{\nu}_e p \to e^+ n$.
  - Prompt e^+ energy $E_{\mathrm{vis}} \approx E_\nu - 0.78\ \mathrm{MeV}$
  - Delayed $np \to d\gamma$ ($E_\gamma = 2.22$ MeV, $\tau \sim 256\ \mu\mathrm{s}$)

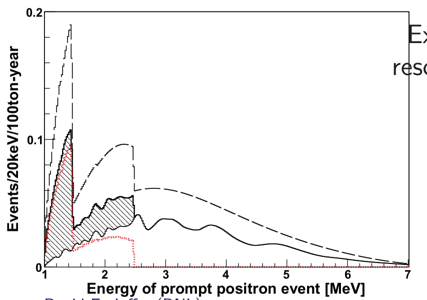

Expected prompt spectrum (without energy resolution)

Dashed	Geo-$\bar{\nu}_e$ & reactor $\bar{\nu}_e$ (no osc.)
Thick	Geo-$\bar{\nu}_e$ & reactor $\bar{\nu}_e$ (with osc.)
Red	Geo-$\bar{\nu}_e$ only

Borexino: Geo-neutrino results

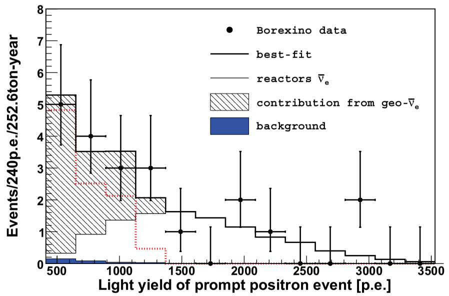

Source	Bkg evts $(100\ \mathrm{ton}\cdot\mathrm{yr})^{-1}$
^{9}Li–^{8}He	0.03±0.02
Fast *n*'s (WT μs)	<0.01
Fast *n*'s (Rock μs)	<0.04
Untagged muons	0.011±0.001
Accid. coinc.	0.080±0.001
Time corr. bkgd	<0.026
(γ,n)	<0.003
Fission in PMTs	0.0030±0.0003
(α,n) in scintillator	0.021±0.002
(α,n) in the buffer	<0.061
Total	0.15±0.02

$N_{\rm geo} = 9.9^{+4.1}_{-3.4}$ ($N_{\rm geo} > 0$ at 99.997% CL) and $N_{\rm reac} = 10.7^{+4.3}_{-3.4}$ events

Consistent with Maximal Radiogenic Earth model: All terrestrial heat produced exclusively by radiogenic elements.

Neutrinos from the Sun

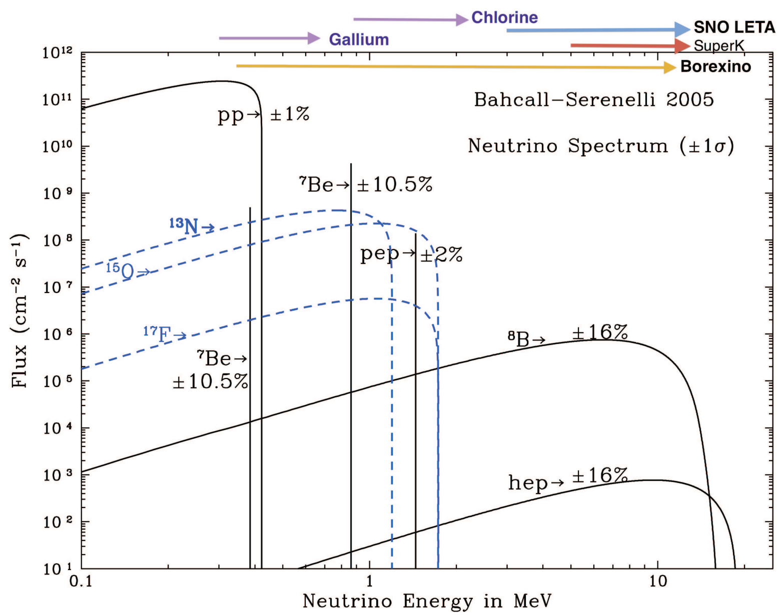

Borexino $^{8}\mathrm{B}$ flux measurement (arXiv:0808.2868v3)

- Solar neutrinos are detected by $\nu e^- \rightarrow \nu e^-$ elastic scattering (ES) in Borexino's liquid scintillator. $\sigma_{\mathrm{ES}}(\nu_e e) \approx \sigma_{\mathrm{ES}}(\nu_{\mu,\tau} e)$.
- A 3 MeV threshold limits background from radioactivity.
- Background is dominated by cosmogenic production of unstable isotopes from $^{12}\mathrm{C}$. ($\sim$4300 muons/day deposit energy in Borexino inner detector)
- Short-lived isotopes are suppressed by a $> 6.5\mathrm{s}$ veto after a muon.
- Longer-lived isotopes ($^{10}\mathrm{C}$, $^{11}\mathrm{Be}$) are suppressed and subtracted.
- From 345.5 live days with a 100t fiducial mass, 75 ± 13 $^{8}\mathrm{B}$ solar ν candidates remain (Solar models: 86 ± 10 or 73 ± 7)

Borexino $^7\mathrm{Be}$ flux measurement (PRL **101**, 091302 (2008))

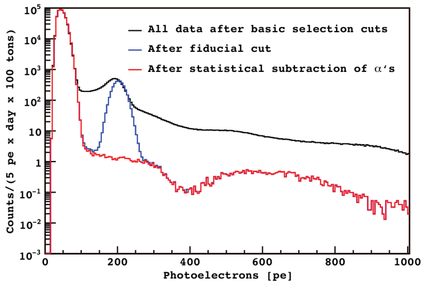

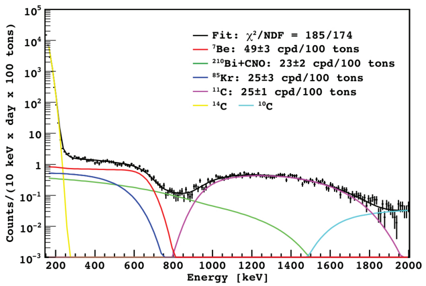

- Signature of monoenergetic 0.862 MeV $^7\mathrm{Be}$ neutrino is Compton-like edge of the recoil electrons at 665 keV
- Suppression of radioactive backgrounds requires outer 2/3 of scintillator to serve as an active shield yielding a 78.5t fiducial mass.
- α background from $^{210}\mathrm{Po}$ at $\sim$400 keV statistically subtracted using pulse-shape discrimination

Resolving the sign of Δm^2_{21} with solar neutrinos

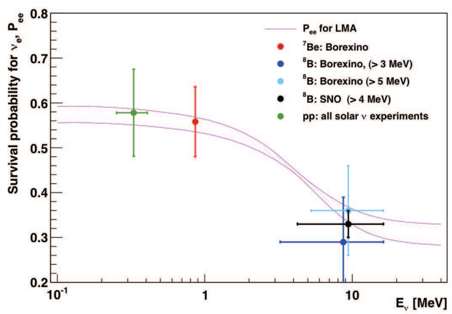

$$\mathcal{H} = \mathcal{H}_{\rm vac} + \mathcal{H}_{\rm matter}(r) = \frac{\Delta m^2_{21}}{4E}\begin{bmatrix} -\cos 2\theta & \sin 2\theta \\ \sin 2\theta & \cos 2\theta \end{bmatrix} + \begin{bmatrix} V(r) & 0 \\ 0 & 0 \end{bmatrix}$$

$$V(0) \approx 0.75 \times 10^{-5}\ {\rm eV}^2/{\rm MeV} \qquad \Delta m^2_{21} = 7.6 \times 10^{-5}\ {\rm eV}^2$$

Sudbury Neutrino Observatory arXiv:0910.2984

- Located in Creighton Mine,CA, 5890 m.w.e. overburden
- 1000 t $\mathrm{D_2O}$ in 12m diam., 5cm thick acrylic vessel
- 9456 20 cm PMTs mounted on 18m diameter steel frame in 8400 t $\mathrm{H_2O}$
- Extensive calibration system
- Solar neutrino detection [a]

  CC $\nu_e + d \rightarrow p + p + e^-$
  ES $\nu_x + e^- \rightarrow \nu_x + e^-$
  NC $\nu_x + d \rightarrow p + n + \nu'_x$
- Phase **I**: "$\mathrm{D_2O}$" (resolved solar ν problem)
- Phase **II**: "Salt phase", +2t NaCl

[a] H.H.Chen, PRL**55** (1985) 1534

SNO: Low-Energy-Threshold Analysis(LETA)

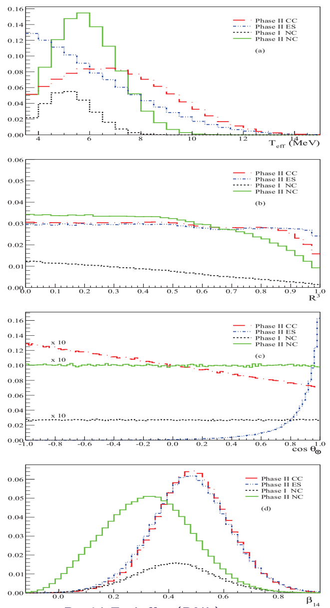

Previous threshold ∼5 MeV, LETA 3.5 MeV

- CC $\nu_e + d \rightarrow p + p + e^-$
- ES $\nu_x + e^- \rightarrow \nu_x + e^-$
- NC $\nu_x + d \rightarrow p + n + \nu'_x$ Phase I (nd)
- NC $\nu_x + d \rightarrow p + n + \nu'_x$ Phase II (nCl)

$T_{\rm eff}$ = effective electron kinetic energy
$R^3 = (R_{\rm fit}/R_{\rm AV})^3$
$\cos\theta_{\odot}$ = direction wrt ν from Sun
β_{14} = 'isotropy' (small β_{14} = high isotropy)

LETA improvements:

1. A more sophisticated energy reconstruction narrowed the resolution by ∼6%, reducing the low-energy backgrounds by ∼60%.
2. Better background rejection cuts
3. Better data quality cuts

Results of SNO LETA (1)

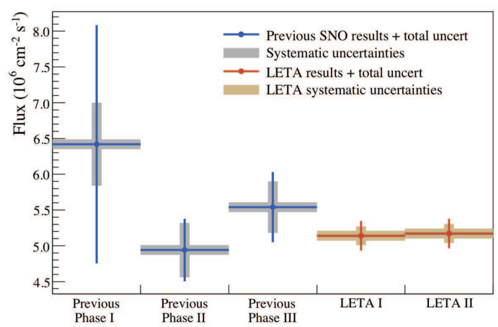

Total $^8\mathrm{B}$ neutrino flux LETA results using the NC ($\nu_x d \rightarrow pn\nu_x$)reaction compared to previous results.

Assuming unitarity, the NC, CC and ES measurements can be combined to yield the most precise measurement of the solar $^8\mathrm{B}$ neutrino flux:

$$\Phi(^8\mathrm{B}) = (5.046^{+0.159}_{-0.152}(\mathrm{stat})^{+0.107}_{-0.123}(\mathrm{syst})) \times 10^6/\mathrm{cm/s}$$

Results of SNO LETA (2)

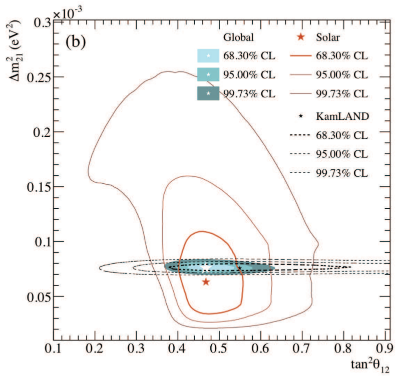

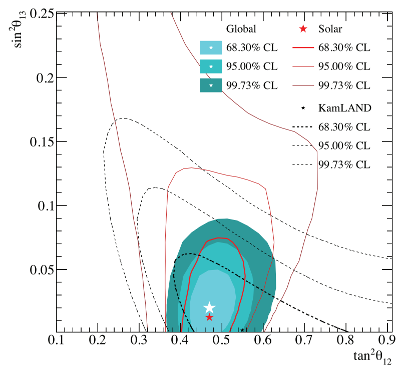

Results of 3ν fit to solar + KamLAND data. (Solar: SNO, Cl, SAGE, Gallex/GNO, Borexino, SK)

$$\theta_{12} = 34.06^{+1.16}_{-0.84}{}^{\circ} \qquad \Delta m^2_{21} = (7.59^{+0.20}_{-0.21}) \times 10^{-5}\ \mathrm{eV}^2$$

$$\sin^2\theta_{13} = (2.00^{+2.09}_{-1.63}) \times 10^{-2} \ \text{ or } \ < 0.057 \text{ at } 95\% \text{ CL}$$

Atmospheric neutrinos and Super-Kamiokande

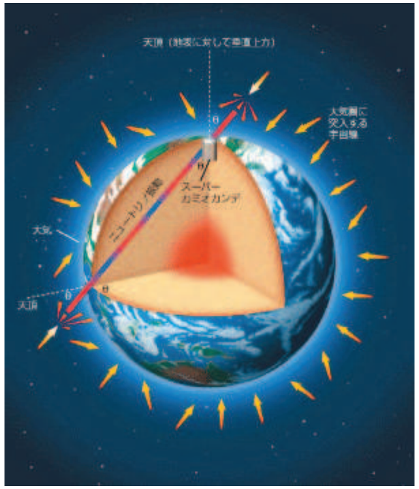

$\pi \longrightarrow \mu\nu_\mu \;\; \mu \longrightarrow e\nu_e\bar{\nu}_\mu$

$N(\nu_\mu) \approx 2N(\nu_e)$

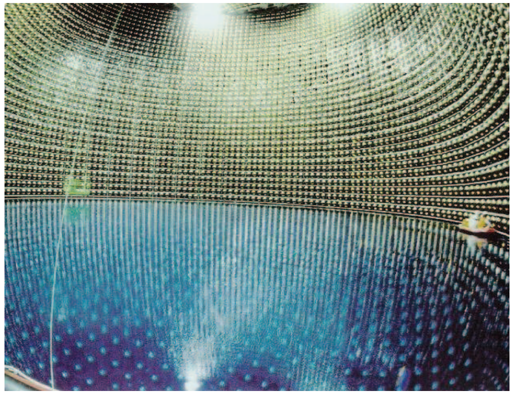

Super-Kamiokande:
cylinder with 39m diam., 41m h.
50kt ultra pure water
2700 mwe overburden
$\sim$11000 20" PMTs ($\sim$40% coverage)

Particle identification in SuperK

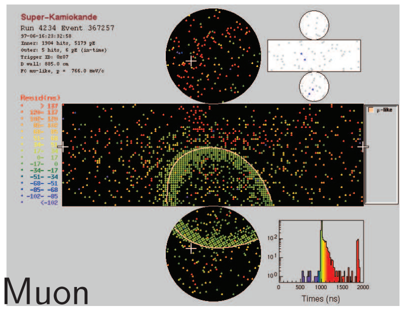

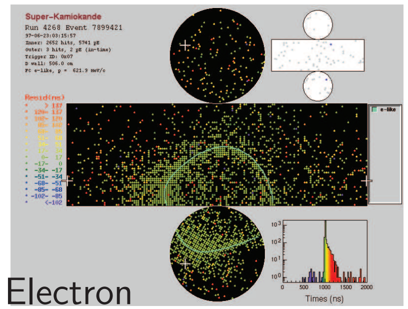

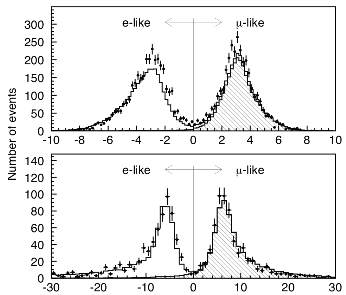

Atmos. ν osc. analysis with sub-leading effects (arXiv:1002.3471)

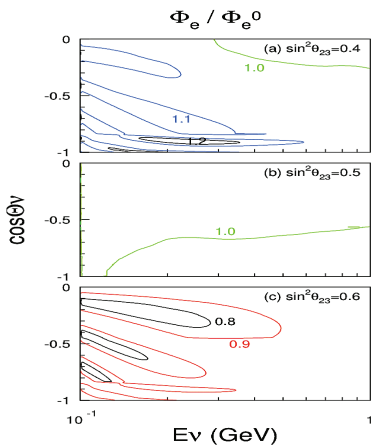

Change in ν_e flux as a function of neutrino zenith angle and energy assuming $\theta_{13} = 0$.

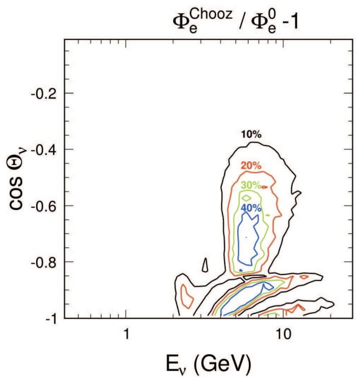

Change in ν_e flux as a function of neutrino zenith angle and energy for θ_{13} at 90%CL upper limit with $\Delta m^2_{23} = 0.0021\ \mathrm{eV}^2$, $\sin^2\theta_{23} = 0.5$, normal hierarchy.

Sub-leading effects in atm. ν in SuperK: Results

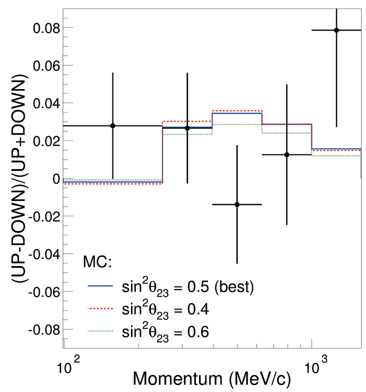

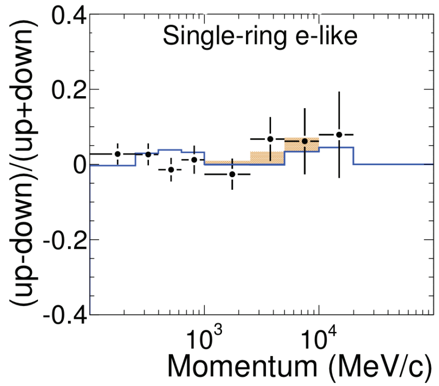

Fit assuming $\theta_{13} = 0$:
$0.407 < \sin^2\theta_{23} < 0.583$
(90%CL).

	$\sin^2\theta_{13}$ (90%CL)	Δm^2 eV^2	$\sin^2\theta_{23}$	$\frac{\chi^2}{\mathrm{DOF}}$
NH	< 0.04	0.0021	0.50	468.7/417
IH	< 0.09	0.0021	0.53	468.4/417

MINOS beam and detectors

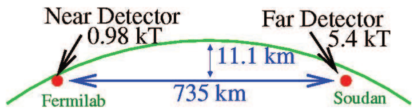

A ~3 GeV ν beam (93% ν_μ, 6% $\bar{\nu}_\mu$, 1% $\nu_e + \bar{\nu}_e$) sent from FNAL to Soudan. MINOS Near (100m depth) and Far (700m depth) Detectors are alternating layers of magnetized steel (2.54cm, 1.4 X_0) and scintillator strips (4.1cm wide).

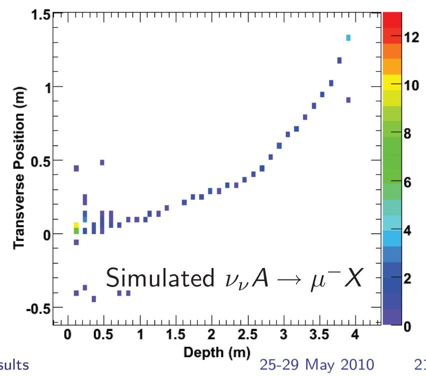

$\nu_\mu \longrightarrow \nu_e$ with matter effect

$$
\begin{aligned}
P(\nu_\mu \to \nu_e) \quad \approx \quad & \sin^2 2\theta_{13} \sin 2\theta_{23} \frac{\sin^2 (A-1)\Delta}{(A-1)^2} \\
& -8\alpha (J \sin\Delta - I \cos\Delta) \frac{\sin A\Delta \sin(1-A)\Delta}{A(1-A)} \\
& +\alpha^2 \cos^2\theta_{23} \sin^2 2\theta_{12} \frac{\sin^2 A\Delta}{A^2}
\end{aligned}
$$

$\alpha \equiv \Delta m^2_{21} / \Delta m^2_{31} \approx 0.03 \qquad \Delta \equiv \Delta m^2_{31} L/4E$
$A = 2VE/\Delta m^2_{31} \approx (E_\nu / 11 GeV)$ for earth's crust
$J \equiv Im(V_{ij} V_{kl} V^*_{kj} V^*_{il}) = \frac{1}{8} \sin\delta \cos\theta_{13} \sin 2\theta_{12} \sin 2\theta_{23} \sin 2\theta_{13}$
$I \equiv Re(V_{ij} V_{kl} V^*_{kj} V^*_{il}) = \frac{1}{8} \cos\delta \cos\theta_{13} \sin 2\theta_{12} \sin 2\theta_{23} \sin 2\theta_{13}$

ν_e appearance probability depends not only on θ_{13} but also on δ and the sign of Δm^2_{31} (the mass hierarchy)

MINOS ν_e appearance: Signal and background

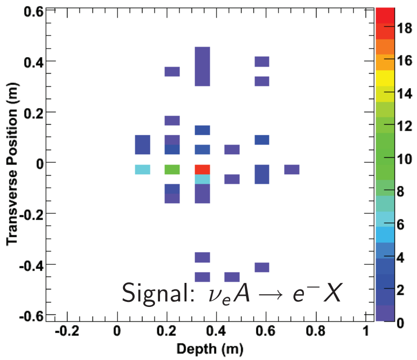

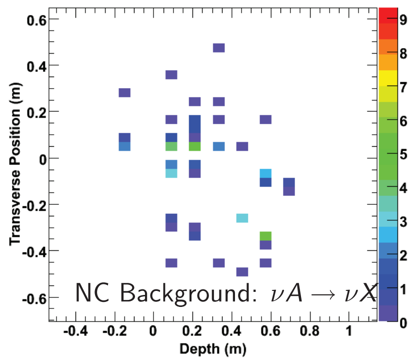

- Other background: ν_μ CC with short μ track, intrinsic beam ν_e, $\nu_\mu \to \nu_\tau$.
- Use artificial neural network (ANN) with 11 shower shape variables to discriminate signal and background.
- Utilize near detector to obtain a background sample and extrapolate to predict the far detector background.

MINOS ν_e appearance: Result (7×10^{20} POT, to be submitted to PRL)

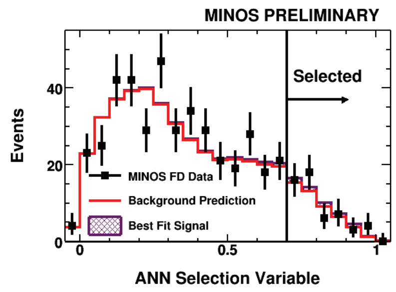

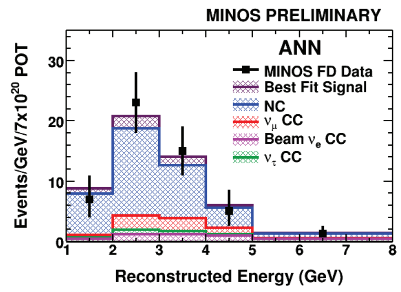

Component	Events
NC	36
ν_μ CC	6
Beam ν_e	5
ν_τ CC	2
Total Bkgd	49.1 ± 7.5
Observation	54

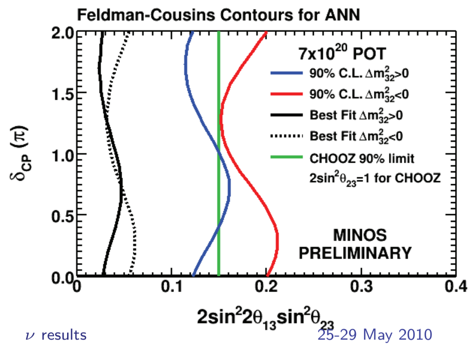

Global fit

- Global analysis of Gonzalez-Garcia, Maltoni and Salvado (arXiv:1001.4524). Similar results from other analyses: arXiv:0905.3546, arXiv:1003.5800
- Uses Borexino, SNO LETA, SuperK and MINOS data shown in this talk.
- Also includes Chlorine, Gallex/GNO, SAGE radiochemical experiments, SuperK solar neutrino results and KamLAND.
- Includes uncertainties due to ν_e capture cross-section in gallium and in the solar model (low- and high-metallicity).

Global fit: Results

$$\Delta m^2_{21} = (7.59^{+0.61}_{-0.69}) \times 10^{-5}\ \mathrm{eV}^2$$

$$\Delta m^2_{31} = \begin{cases} (-2.36 \pm 0.37) \times 10^{-3}\ \mathrm{eV}^2 \\ (+2.46 \pm 0.37) \times 10^{-3}\ \mathrm{eV}^2 \end{cases}$$

$$\theta_{12} = (34.4^{+3.2}_{-2.9})^\circ$$
$$\theta_{23} = (42.8^{+10.7}_{-7.3})^\circ$$
$$\theta_{13} \le 12.5^\circ$$
$$\delta_{\mathrm{CP}} \in [0,\ 360]^\circ$$

(Uncertainties, limits are at 3σ)

Different contours correspond to 90%, 95%, 99% and 3σ CL.

Full regions: High-metallicity solar model.

Void regions: Low-metallicity solar model.

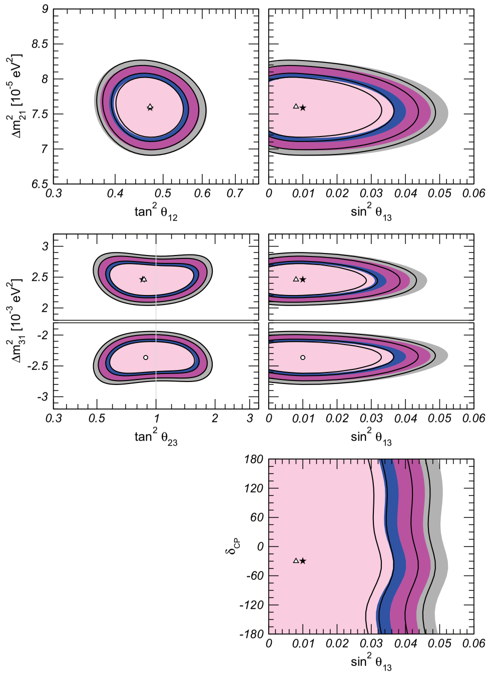

Vague prognostications

1. 2-3 mixing is nearly maximal. θ_{23} might be 45°.
2. θ_{13} is small. It might be zero.
3. I predict the next two speakers will try to tell us when we will know
   - 3.1 θ_{13},
   - 3.2 the mass hierarchy,
   - 3.3 the mass of the neutrino,
   - 3.4 if CP is violated for leptons, and
   - 3.5 if neutrinos are their own anti-particles.

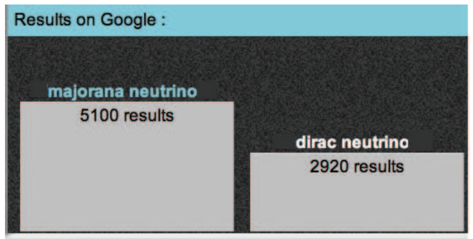

Thanks to Michael Sivertz and Brett Viren for comments on these slides.

Additional slides

SNO LETA

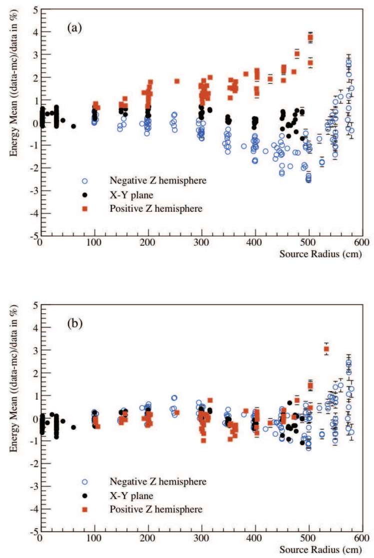

Energy reconstruction algorithm improved by inclusion of scattered and reflected Čerenkov light.
Validated by extensive comparison of calibration data and simulated data.
Calibration sources: Laser, $^{16}\mathrm{N}$, $^{8}\mathrm{Li}$, $^{252}\mathrm{Cf}$, Am-Be, cosmogenic neutrons, etc.
Figure: Difference in $^{16}\mathrm{N}$ data and MC energy scale *vs.* radius. (a) before and (b) after spatial energy correction.

χ^2 *vs* $\sin^2 \theta_{13}$